DEPTH TRENDS IN CHEMCAM LIBS DATA IN THE SULFATE BEARING UNIT K. Rammelkamp[1], O. Gasnault[2], S. Schröder[1], A. Lomashvili[1], E. B. Hughes[3]; [1]German Aerospace Center (DLR), Institute of Optical Sensor Systems, Berlin, Germany; [2]Institut de Recherches en Astrophysique et Planétologie, Toulouse, France; [3]Georgia Institute of Technology, USA; (kristin.rammelkamp@dlr.de)

Introduction: In 2012, NASA's Mars Science Laboratory started its journey through Gale crater, Mars. One instrument of the payload is ChemCam which uses LIBS (laser-induced breakdown spectroscopy) to analyze the chemical composition of martian rocks and soils [1,2]. With a pulsed laser, material is ablated from the surface of the sample, which then forms a plasma. The plasma contains excited atoms, ions and simple molecules that emit characteristic radiation. By analyzing this radiation spectroscopically, the composition of the sample can be determined. ChemCam typically creates a raster of 5 measuring points on a target (since sol 3007, prior to that 10 points were typically acquired), each of which is subjected to 30 laser pulses, i.e. 30 LIBS plasmas are created one after the other, and the radiation of each is recorded. Standard ChemCam LIBS data processing averages the spectra, excluding the first 5 to avoid dust contribution, and uses multivariate calibration to determine the geochemical composition at the point of measurement [3]. The aim of this study is to explore ChemCam LIBS data from the sulfate bearing unit (SBU) using an unsupervised decomposition technique, in which all 30 spectra of a measurement point are taken into account. The idea is that this also accounts for trends with the depth of the LIBS crater as with each laser shot, material slightly deeper is ablated. The 30 laser shots can produce different depths, depending on the material properties of the target, but typically the average depth can be expected to be about 100 μm [4]. Correlations of element emission lines over successive shots can provide support for mineral identification, assuming that the elements belong predominantly to one mineral phase [5]. A method from the field of tensor component analysis (TCA) will be used, which extends matrix decomposition techniques to more than two dimensions [6]. TCA has previously been applied to ChemCam LIBS data from samples with a predominantly felsic composition, demonstrating the potential of this method for identifying more detailed mineral and depth trends [7].

Method: There are two main approaches to multiway tensor decomposition: the Tucker decomposition and parallel factor analysis (PARAFAC) [6], the latter being used in this study. The typical data matrix of ChemCam LIBS points and spectrum (wavelength, 6144 channels) is extended by a third dimension associated to the shots (here: 30). In brief, the basic idea is to decompose the tensor in a sum of rank one tensors [6], the number of which R needs to be fixed in advance. With ChemCam LIBS data, each rank-one tensor, which we will also refer to as a factor, has dimensions corresponding to observation points, consecutive shots (depth), and wavelength (spectra). We use non-negative PARAFAC so that all values are restricted to be > 0. For the computation, the hierarchical alternating least squares (HALS) algorithm provided in python's TensorLy [8] package was utilized.

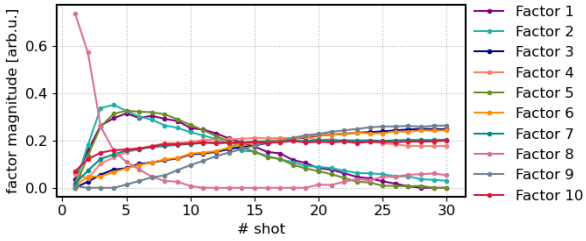

Figure 1: *Depth trends of all 10 factors shown as a function of shot number.*

Data: In this study, we analyze recent ChemCam data from the sulfate bearing unit (sol 3597-4037) with TCA, omitting data measured during a detour to the Gediz Vallis deposits (sol 3638-3690) and that of the marker bed (sol 3709-3771). The compositions in this region show strong contributions from salts such as Ca- and Mg-sulfates as well as halite. In total, shot-to-shot data from 1275 observation points are analyzed, resulting in a data tensor with dimensions of $1275 \times 30 \times 6144$.

Results:

We computed models with 3-14 ranks and decided for the one with 10 ranks based on a reconstruction error $< 10\,\%$ and no further significant decrease with more ranks. We cannot provide a detailed analysis of each of the 10 factors here. Instead, we offer general observations and a rough interpretation of each factor below. Fig. 1 displays the depth dimension and Fig. 2 shows the spectral dimension of all factors, while both the trends and main spectral signatures are summarized in Table 1. Overall, it is noticeable that three factors exhibit a similar trend with depth, initially increasing and then decreasing (factors 1, 2, 5). Upon examining the spectral dimensions of these factors, it becomes apparent that each factor has a corresponding partner with an almost identical spectral dimension. These pairs are as follows: Factor 1 and 3 with strong Mg, 2 and 6 with strong Fe, and 5 and 9 with strong Ca emission lines. With depth, the partner factors 3, 6 and 9 have opposite trends, i.e. they increase with depth. All three pairs show a pairwise correlation of their values in the obser-

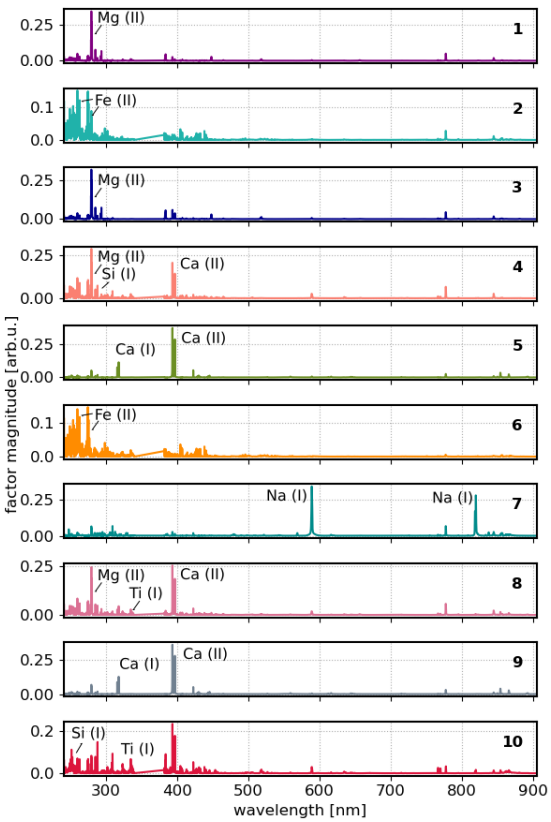

Figure 2: *Spectral dimension of all 10 factors. Strongest and characteristic emission lines were annotated.*

vation points dimension. This means that observation points, for example, with a high value on factor 3 (Mg, ↑) also have a high value on factor 1 (Mg, ↓). It can be interpreted that the two opposing trends add up at most observation points, resulting in a constant level of the corresponding element after dust removal. However, some observation points deviate from this correlation, showing either a decreasing or increasing trend for the element with depth. Moreover, transitions between the elements of the three pairs (Mg, Fe, Ca) can be identified. For example, some observation points have high values for factors 2 and 3, indicating increasing Mg and decreasing Fe with depth. The spectral dimensions of the Ca and Mg factors also show S emission lines which points to the presence of Ca- and Mg-sulfates. Additionally, factor 1 (Mg, ↓) exhibits a strong H signal, consistent with hydrated Mg-sulfate. This is one of the few differences from factor 3 (Mg, ↑), as its spectral dimension exhibits a somewhat weaker H signal, see Fig. 3. Another factor representing a salt is factor 7 with the spectral dimension (Fig. 2) showing strong Na and Cl emission lines indicating halite. Here only one trend was found by TCA having a short increase during the first 10 shots and then being mostly constant (Fig. 1). The dust contribution is covered with factor 8 with typical emission lines of Mg, Ca, Ti and H [9] and a decreasing trend with shot number. Factor 10 can be assigned to likely GVR float rocks with emission lines mainly in agreement with a Stimson-like composition [10] and enhanced Ti and Cr lines.

Factor	Trend	Main spectral feature
1	short ↑ to ↓	Mg
2	short ↑ to ↓	Fe
3	↑	Mg
4	↑ to →	baseline bedrock
5	short ↑ to ↓	Ca
6	↑	Fe
7	↑ to →	NaCl
8	↓	dust
9	↑	Ca
10	↑ to →	floats

Table 1: *Broad summary of the depth and spectral trends of all 10 factors with ↑: increasing; ↓: decreasing; →:constant.*

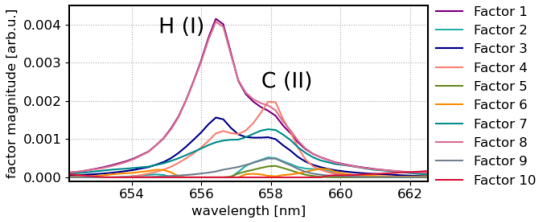

Figure 3: *Zoom to spectral region with H and C emission lines showing all factors. H signal is strongest on factors 1 (Mg, ↓) and 8 (dust).*

Conclusions: As expected, the TCA model is dominated by factors related to salts such as Ca and Mg sulfates and halite. Their factors seem to remain relatively constant with depth, although in some cases, we observe transitions between Ca, Mg and Fe contributions. Based on their appearance on distinct and uncorrelated factors, as well as the occasional transitions with depth, it is likely that these elements do not belong to the same mineral phase for most LIBS observations in SBU.

Outlook: Next, we will investigate the observation point dimension in more detail, mainly the point-to-point variability of individual targets and how their distribution relates to the rover's traverse. Additionally, we will explore the possibility of clustering observation points with similar values on the spectral and depth factors. Further investigation of the TCA itself will be conducted to determine if prior knowledge of the factors or concepts such as regularization can improve the results.

References: [1] Maurice et al. (2012), *SSR*, 170; [2] Wiens et al. (2012), *SSR*, 170; [3] Clegg et al. (2017), *SAP B*, 129, 64; [4] Maurice et al. (2016), *JAAS*, 4; [5] Forni et al. (2018), *LPSC*, #1410; [6] Kolda and Bader (2009), *SIAM*, 51; [7] Rammelkamp et al. (2022), *LPSC*, #1999; [8] Kossaifi et al. (2019), *JMLR*, 20; [9] Lasue et al. (2018), *GRL*, 45; [10] Bedford et al. (2022), *JGR*, 127.